Colloid Polym Sci 279:1236–1240 (2001)

SHORT COMMUNICATION

T. Okubo
T. Miyamoto
K. Umemura
K. Kobayashi

Seed polymerization of tetraethyl orthosilicate in the presence of colloidal silica spheres

Received: 25 January 2001
Accepted: 30 May 2001

T. Okubo (✉) · T. Miyamoto
K. Umemura · K. Kobayashi
Department of Applied Chemistry
and Graduate School of Materials Science
Gifu University, Yanagido 1-1
Gifu 501-1193, Japan
e-mail: okubotsu@apchem.gifu-u.ac.jp
Fax: +81-58-2932628

Abstract Kinetic analyses were made for the seed polymerization of tetraethyl orthosilicate (TEOS) in the presence of colloidal silica sphere seeds by turbidity and dynamic light scattering (DLS) measurements. Transmission electron microscopy (TEM) of the spheres formed was also used. TEOS is polymerized exclusively on the surfaces of the seed spheres, their sizes ranging from 29 to 184 nm in diameter. The sphere size versus time and the cube root of the absorbance versus time from DLS and turbidity measurements agree well, especially in the beginning of the reaction. The seed polymerization starts immediately on the addition of seed spheres, though the polymerization in the absence of the seeds proceeds after a certain induction time ranging several tens of seconds to several minutes. The polymerization rates of the reaction increase when the size and/or the concentration of the seed spheres increases. The thickness of the TEOS layers formed on the seed surfaces increases as the seed size increases; this is confirmed by the TEM pictures. These results are consistent with the polymerization mechanism of the formation of small preliminary particles followed by their coalescence on the surfaces of seeds to the final large spheres coated with silica layers.

Key words Seed polymerization · Turbidity · Dynamic light scattering · Transmission electron microscope

Introduction

Monodisperse colloidal particles of any size and any shape have provided most of the exciting and essential samples for studies in the field of colloidal science. The main purpose of this work was to synthesize hydrophilic and stable colloidal particles of any size and shape. As is well known, colloidal silica spheres are highly hydrophilic and disperse nicely without coagulation in water, especially in the deionized state with the coexistence of mixed beds of cation- and anion-exchange resins. However, syntheses of the monodispersed and nonspherical particles of silica are extremely difficult. The reaction mechanism of the monodispersed, nonspherical and stable colloidal particles was studied in our laboratory by coating the seed particles with silica layers. In this report, the detailed investigation of seed polymerization of tetraethyl orthosilicate (TEOS) on the surfaces of colloidal silica spheres is reported.

There have been significant developments in techniques for colloidal silica synthesis and this have been accompanied by recent advances in the sol–gel method in the field of fine ceramics [1–3]. The synthesis of colloidal silica was first reported by Stober et al. [4] in 1968 and was studied further by several researchers [5–18]. The polymerization reaction is composed of the hydrolysis of silicate, Eq. (1), and then the dehydration is accompanied by three-dimensional cross-linking, Eq. (2).

$$Si(OC_2H_5)_4 + 4H_2O \rightarrow Si(OH)_4 + 4C_2H_5OH \quad (1)$$

$$\equiv SiOH + HO - Si \equiv \rightarrow \equiv Si - O - Si \equiv + H_2O \quad (2)$$

According to Shimohira and coworkers [7, 19] the primary small particles are formed during an induction period, t_i, at the beginning of the reaction. Their critical size was estimated to be 10–20 nm [7]. The growing process with the coalescence of the primary particles then follows, and the final silica spheres are formed.

Shimohira and coworkers proposed that the sixth order of the sphere size increases linearly with the reaction time, Eq. (3),

$$r^6 \propto t \ , \tag{3}$$

where r is the radius of the spheres. It should be recalled that the Lifshitz–Slyozov–Wagner theory supports the second- and third-order relations for the surface reaction-controlled and diffusion-controlled mechanisms, respectively [20]. Furthermore, fourth- and fifth-order relations were proposed for the surface diffusion and the diffusion accompanied by the dislocation in the cases of ceramics and metal formations, respectively [20, 21]. Several experiments, however, supported sixth- or seventh-order relations [22–24], and theoretical explanations for the relationships were not successful. Recently, a small-angle X-ray scattering study [18] revealed that after an induction period the first particles to appear in the solution have a radius of gyration of about 10 nm and are mass fractals characterized by their polymeric open structure. The report did not support the growth model proposed so far by Shimohira and coworkers, for example.

Recent advances in the polymerization reaction of colloidal silica spheres were reviewed by Ogihara [25]. We studied the kinetic mechanism of the formation reaction of colloidal silica spheres from TEOS in normal gravity on the Earth [26] and also in microgravity [27].

Experimental

Materials

Six kinds of colloidal silica spheres were kindly donated by Catalyst & Chemicals Co. (Tokyo). The characteristics of the spheres are compiled in Table 1. Their diameters and the polydispersity indices range from 29 to 184 nm and from 0.04 to 0.21, respectively. The colloidal samples were first purified several times using an ultrafiltration cell (model 202, Diaflo-XM300 membrane, Amicon Co.), and then deionized by a mixed bed of cation- and anion-exchange resins more than 3 years before use. They released an amount of alkali from their surfaces. Thus, it takes a long time for complete deionization, since the deionization proceeds between the two solid–liquid phases stepwise, i.e., between colloidal spheres and water and then between water and the resins. Their diameters (d) were determined through the courtesy of Nippon Synthetic Rubber Co. (Tokyo) by electron microscopy. The standard deviation (δ) of the diameter of each sphere from the mean diameter was determined from the electron microscope pictures of more than 500 spheres. The surface density of strongly acidic groups of these spheres was determined by conductometric titration with a Horiba model DS-14 conductivity meter (Kyoto). Strongly acidic and weakly acidic groups coexisted at the surface of the colloidal silica spheres.

Table 1 Properties of the colloidal silica spheres used as seeds

Spheres	Diameter (d) (nm)	δ (nm)	δ/d	Charge density (μC/cm^2)
CS-22	29	6	0.21	–
CS-45	56.3	7.6	0.13	0.30
CS-82	103	13.2	0.13	0.38
CS-91	110	4.5	0.040	0.48
CS-121	136	10.9	0.080	0.40
CS-161	184	18.6	0.10	0.47

TEOS was purchased from Wako Pure Chemicals (Osaka). Ethanol (99.5%) and ammonia (N25%) were commercially available purified grade reagents and were obtained from Wako Chemicals. The water used for the sample preparation was purified by a Milli-Q reagent grade system (Milli-RO5 plus and Milli-Q plus, Millipore, Bedford, Mass.).

Turbidity and dynamic light scattering measurements

The turbidity, i.e., absorbance at 600 nm, was recorded using a spectrophotometer (Beckmann, DU650). Quartz optical cells (10 mm × 10 mm × 70 mm high) with long necks and screw caps were used for the kinetic turbidity measurements. The seed polymerization was started by adding 1 ml TEOS in ethanol to the mixtures of ammonia and the seed spheres in ethanol. Then, the increase in the absorbance at 680 nm was measured. The change in the effective radii of the colloidal silica spheres including the thickness of the polymerized layers was also determined using a dynamic light scattering (DLS) spectrophotometer (DLS-7000, Otsuka Electronics, Osaka). The reaction mixture of 5 mL was prepared in a Pyrex cuvette (12-mm outside diameter and 130-mm length) with a screw cap. These cuvette cells were ground to a spectroscopic guaranteed level and were very clear.

Transmission electron microscopy

The suspension (0.1 ml) was dried on a collodion mesh at room temperature before the transmission microscopy (Hitachi, H8100).

Results and discussion

Size, induction periods, and polymerization rates from turbidity measurements

A typical example of the turbidity measurements is shown in Fig. 1. The volume fraction of the seed spheres ranges from 0 to 0.001. The total absorbance (A) consists of the solvent absorption (A_o), the absorption from the particle formed (A_p), and the light scattering at θ (scattering angle) = 0 (A_s), i.e., Eq. (4) [4].

$$A = A_o + A_p - A_s \tag{4}$$

The A_p term arising from the colloidal spheres formed in the seed polymerization should increase linearly with increasing volume of the sphere as

$$A_p \propto Nr^3 \ , \tag{5}$$

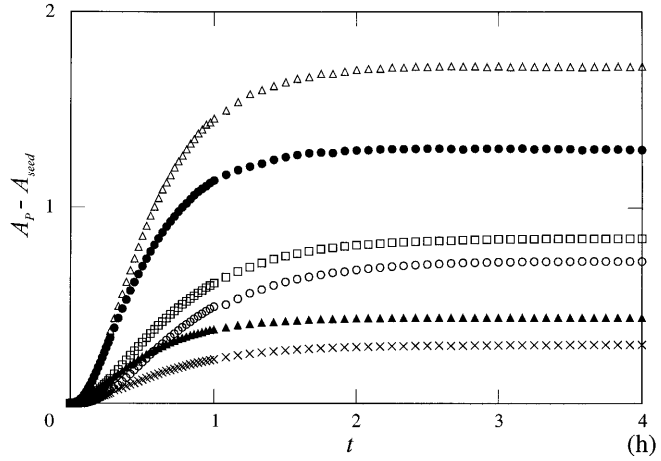

Fig. 1 Absorbance at 600 nm in the course of seed polymerization of tetraethyl orthosilicate (*TEOS*) in the presence of CS-82 spheres at 25 °C. [TEOS] = 0.5 vol%, [NH_3] = 3.0 wt%. $\phi_{CS\text{-}82} = 0$ (○); 1×10^{-5} (×); 5×10^{-5} (△); 1×10^{-4} (□); 5×10^{-4} (●); 1×10^{-3} (◆)

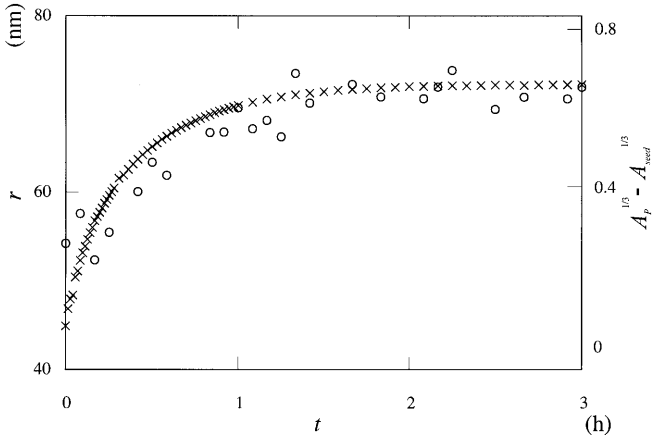

Fig. 3 Comparison of the radii from dynamic light scattering (*DLS*) (○) and turbidity (×) measurements during seed polymerization at 25 °C. [TEOS] = 0.5 vol%, [NH_3] = 3.0 wt%, $\phi_{CS\text{-}82} = 0.001$

where N is the number of the spheres formed and r is the diameter of the spheres. Equation (6) is derived from Eq. (5):

$$A_p = A_{shell} + A_{seed} \propto r^3 \quad , \tag{6}$$

where A_{shell} and A_{seed} denote the absorbance contribution of the silica layers and from the seeds themselves.

It should be noted here that Eq. (4) holds only if the absorption dominates the scattering. If the scattering dominates, $A_p \propto Nr^6$. The light scattering term, A_s, is further approximated by Eq. (7):

$$A_s \propto \ln(I_p \times I_i + I_m) \quad , \tag{7}$$

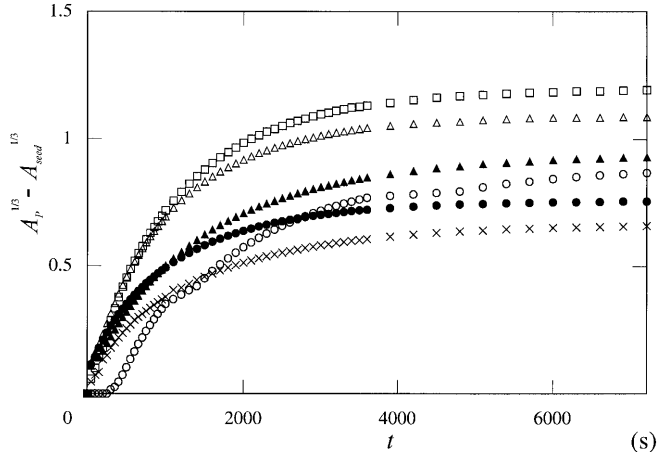

Fig. 2 Absorbance at 600 nm for the seed polymerization at 25 °C. [TEOS] = 0.5 vol%, [NH_3] = 3.0 wt%. $\phi_{CS\text{-}82} = 0$ (○); 1×10^{-5} (×); 5×10^{-5} (△); 1×10^{-4} (□); 5×10^{-4} (●); 1×10^{-3} (◆)

where I_p is the intensity of the scattered light from the particle form factor at $\theta = 0$. I_i is the intensity of scattered light related to the interference factor at $\theta = 0$. This term reflects the particle distribution in the reaction mixtures. I_m is the multiple-scattering term and is especially important in the final stage of the polymerization reaction where large colloidal spheres grow. The radius, r, and the reaction rate, v, are, therefore, approximated very roughly by Eqs. (8) and (9), especially at the beginning of the polymerization reaction. However, it is highly plausible that the densities of the seed and the shell layer differ and the absorption should change with time; thus, we note that the analyses using Eqs. (8) and (9) are not so reliable and lead to rather large errors:

$$r \propto A_p^{1/3} \quad , \tag{8}$$

$$v = dr/dt \propto dA_p^{1/3}/dt \quad . \tag{9}$$

$A_p^{1/3} - A_{seed}^{1/3}$ is shown as a function of time in Fig. 2. The induction time, t_i, was zero in the presence of seed silica spheres, irrespective of the seed concentration though the induction time was observed in the absence of the seed spheres. This observation supports the idea that the polymerization of TEOS proceeds exclusively on the surface of the seed spheres.

The polymerization rates of TEOS were estimated from the final thickness of the silica layers determined from the DLS measurements and from the reciprocal period between the intersections of the linear line with the initial and final horizontal lines in the cube root of A_p versus time plots. It should be noted here that the seed polymerization should be made at TEOS volume fractions below 0.2, where TEOS dissolves homogeneously in ethanol.

Size versus time profiles from DLS measurements

A plot of the diameter from the DLS and the cube root of A_p from the turbidity methods is shown in Fig. 3. Again, the values of r from the turbidity method are not so reliable since the method contains several assumptions as described previously. On the other hand, the DLS technique directly gives the size data; however, the accuracy of the DLS measurements was rather low compared with that of the aqueous suspensions. Agreement of the sizes from both measurements was excellent.

The thickness of the silica shell, r_{shell} $(=r-r_{seed})$ estimated from the DLS measurements is shown by open circles as a function of the size of the seeds (Fig. 4); r_{shell} increased with r_{seed}. As the volume fraction of the seeds is fixed, the total surface area of the seeds is given by $4\pi r_{seed}^2 \times 0.001/[(4/3)\pi r_{seed}^3]$ and should increase with the reciprocal of the diameter of the seed spheres; thus, the thickness of the shell layers should increase as the sphere size increases, since the total area becomes small for the large spheres.

The polymerization rate estimated from the turbidity and DLS measurements is shown as a function of the size of the seed spheres in Fig. 5. The growth rates of the shell layers increased as the concentration and/or the size of the seed spheres increased. These results are quite consistent with the reaction mechanism that the very

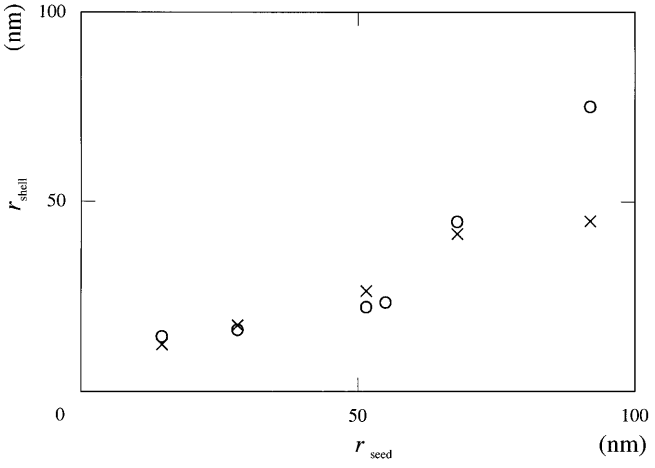

Fig. 4 Thickness of the shell layers (r_{shell}) estimated from DLS (○) and turbidity (×) measurements at 25 °C. [TEOS] = 0.5 vol%, [NH_3] = 3.0 wt%, $\phi_{seed} = 0.001$

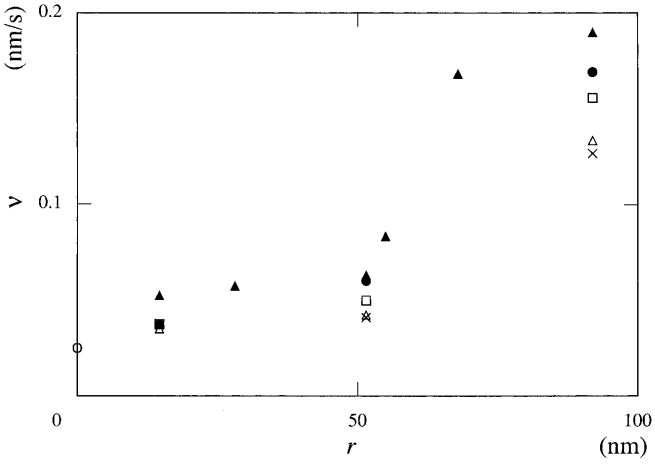

Fig. 5 Polymerization rates of TEOS from turbidity measurements at 25 °C. [TEOS] = 0.5 vol%, [NH_3] = 3.0 wt%. $\phi_{seed} = 0$ (○); 1×10^{-5} (×); 5×10^{-5} (△); 1×10^{-4} (□); 5×10^{-4} (●); 1×10^{-3} (◆)

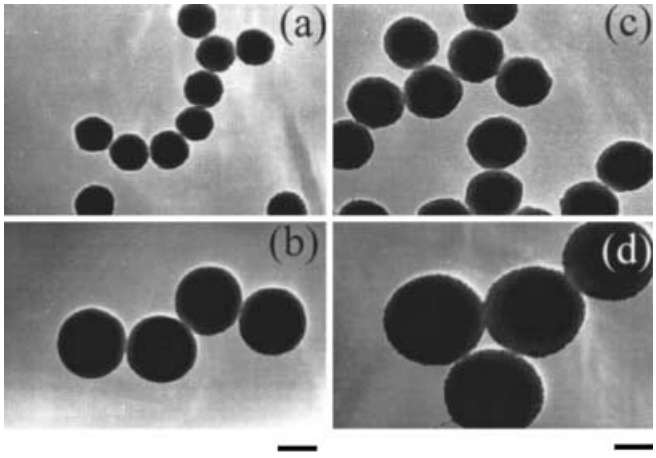

Fig. 6a–d Transmission electron microscopy (*TEM*) pictures of CS-45 or CS-82 seed spheres. **a** Before polymerization, $\phi_{CS\text{-}45} = 1 \times 10^{-3}$, length of the bar: 150 nm. **b** After polymerization, $\phi_{CS\text{-}45} = 1 \times 10^{-3}$, length of the bar: 150 nm. **c** Before polymerization, $\phi_{CS\text{-}82} = 1 \times 10^{-3}$, length of the bar: 100 nm. **d** After polymerization, $\phi_{CS\text{-}82} = 1 \times 10^{-3}$, length of the bar: 100 nm

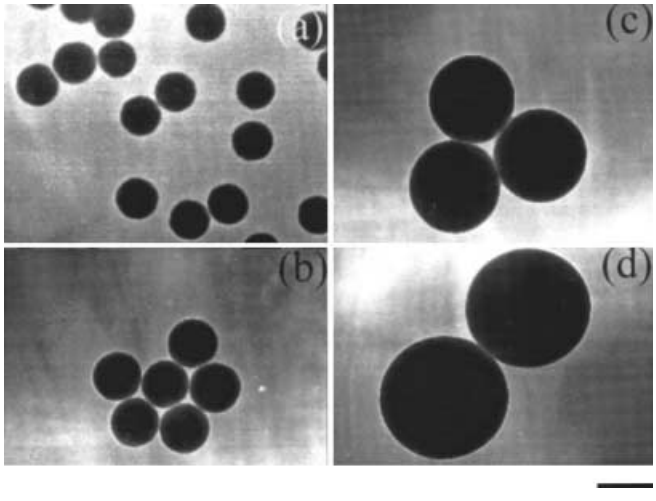

Fig. 7a–d TEM pictures of CS-121. **a** Before polymerization, **b** after polymerization, $\phi_{CS\text{-}121} = 1 \times 10^{-3}$, **c** after polymerization, $\phi_{CS\text{-}121} = 1 \times 10^{-4}$, and **d** after polymerization, $\phi_{CS\text{-}121} = 1 \times 10^{-5}$. The length of the bar is 200 nm

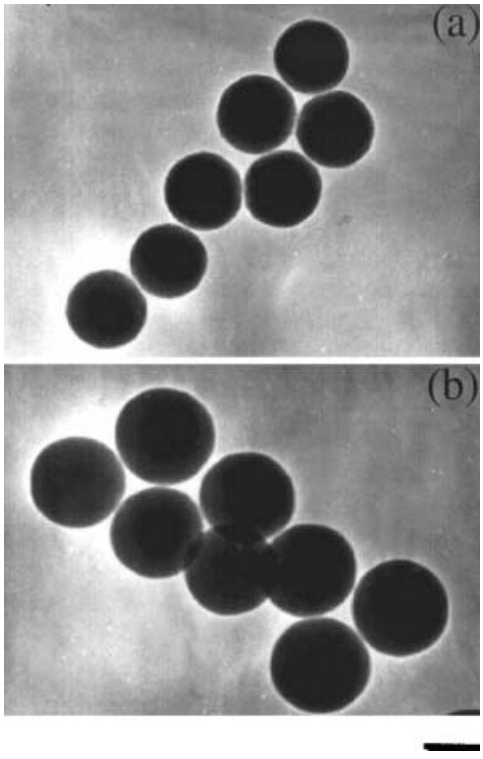

Fig. 8a, b TEM pictures of CS-161. $\phi_{\text{CS-161}} = 1 \times 10^{-4}$. **a** Before polymerization and **b** after polymerization. The length of the bar is 200 nm

small preliminary particles are formed first and then coalesce. Since the chemical composition of the seeds and the preliminary particles is identical, the affinity between the seeds and the preliminary particles must be so strong that the coalescence and shell formation occur exclusively on the surfaces of the seeds.

Transmission electron microscopy observation

Figure 6 shows the transmission electron microscopy (TEM) pictures of the spheres before and after polymerization in the presence of CS-45 (Fig. 6a, b) and CS-82 spheres (Fig. 6c, d). All the seed spheres were coated with a homogeneous silica shell. Small preliminary particles are seen on the surface of the particles in Fig. 6d.

TEM pictures of the spheres in the presence of various amounts of seed spheres are shown in Fig. 7. The size of the spheres formed increased when the concentration of the seed spheres decreased. This observation is consistent with the change in the molecular weight of polymers by the radical polymerization: the molecular weight increases when the concentration of the initiator decreases. Here, the thicknesses of the silica layers and the seed are related to the molecular weight and the initiator, respectively. TEM pictures of the largest spheres formed in the presence of CS-161 spheres are shown in Fig. 8. Shell formation is also clearly observed.

The r_{shell} values of the layers of silica around the seed particles were calculated from the TEM pictures (Fig. 6). Surprisingly, the values from the DLS and TEM techniques agreed very well. This suggests strongly that silica layers are very rigid and that the size of the spheres does not change on drying in the TEM measurements.

Acknowledgements M. Komatsu and M. Hirai of Catalysts & Chemicals Ind. Co. (Tokyo and Kitakyusyu) are thanked for providing the silica spheres. The Ministry of Education, Science, Sports and Culture is thanked for Grants-in-Aid for Scientific Research on Priority Area (A) (11167241) and for Scientific Research (B) (11450367). T.O. appreciates greatly the late Professor Emeritus Sei Hachisu for his continual encouragement and comments on our work.

References

1. Iler RK (1979) The chemistry of silica. Wiley, New York
2. Klein LC (ed) (1988) Sol–gel technology for thin films, fibers, preforms, electronics and specialty shapes. Noyes, Park Ridge, NJ
3. Bergna HE (1994) The colloid chemistry of silica. American Chemical Society, Washington, DC
4. Stober W, Fink A, Bohn E (1968) J Colloid Interface Sci 26:62
5. van Helden AK, Vrij A (1980) J Colloid Interface Sci 78:312
6. Kops-Werkhoven MM, Fijnant HM (1980) In: Degiorgio V, Corti M, Giglio M (eds) Light scattering in liquids and macromolecular solutions. Plenum, New York, p 81
7. Shimohira T, Ishijima J (1981) Jpn J Chem Soc 1503
8. Okubo T (1988) J Chem Phys 88:6581
9. Matsoukas T, Gulari E (1988) J Colloid Interface Sci 124:252
10. Matsoukas T, Gulari E (1989) J Colloid Interface Sci 132:13
11. Bogush GH, Zukoski CF IV (1991) J Colloid Interface Sci 142:1
12. Bogush GH, Zukoski CF (IV 1991) J Colloid Interface Sci 142:19
13. van Blaaderen A, van Geest J, Vrij A (1992) J Colloid Interface Sci 154:481
14. van Blaaderen A, Kentgens APM (1992) J Non-Cryst Solids 149:161
15. Okubo T (1992) Ber Bunsenges Phys Chem 96:61
16. Giesche H (1994) J Eur Ceram Soc 14:189
17. Lee K, Look JL, Harris MT, Mc Cormick AV (1997) J Colloid Interface Sci 194:78
18. Boukari H, Lin JS, Harris MT (1997) J Colloid Interface Sci 194:311
19. Shimohira T, Komuro N (1976) Powder Metall 23:137
20. Shewnon PG (1964) Trans Metall Soc AIME 230:1134
21. Nichols FA (1966) J Appl Phys 37:4599
22. Heg AW, Livey DT (1966) Trans Br Ceram Soc 65:626
23. Kotera Y, Saito T, Terada M (1963) Bull Chem Soc Jpn 36:2195
24. Aihara K, Chaklader ACD (1975) Acta Metall 23:855
25. Ogihara T (2000) In: Sugimoto T (ed) Fine particles. Synthesis, characterization, and mechanisms of growth. Dekker, New York, p 35
26. Okubo T, Kobayashi K, Kuno A, Tsuchida A (1999) Colloid Polym Sci 277:483
27. Okubo T, Tsuchida A, Kobayashi K, Kuno A, Morita T, Fujishima M, Kohno Y (1999) Colloid Polym Sci 277:474